NIH Public Access
Author Manuscript
*J Phys Chem B*. Author manuscript; available in PMC 2014 September 12.

Published in final edited form as:
*J Phys Chem B*. 2013 September 12; 117(36): 10572–10580. doi:10.1021/jp4061889.

# A Comparative Kirkwood-Buff Study of Aqueous Methanol Solutions Modeled by the CHARMM Additive and Drude Polarizable Force Fields

**Bin Lin**, **Xibing He**, and **Alexander D. MacKerell Jr.***
Department of Pharmaceutical Sciences, University of Maryland, School of Pharmacy, 20 Penn Street HSFII, Baltimore, Maryland 21201, USA

## Abstract

A comparative study on aqueous methanol solutions modeled by the CHARMM additive and Drude polarizable force fields was carried out by employing Kirkwood-Buff analysis. It was shown that both models reproduced the experimental Kirkwood-Buff integrals and excess coordination numbers adequately well over the entire concentration range. The Drude model showed significant improvement over the additive model in solution densities, partial molar volumes, excess molar volumes, concentration-dependent diffusion constants, and dielectric constants. However, the additive model performed somewhat better than the Drude model in reproducing the activity derivative, excess molar Gibbs energy and excess molar enthalpy of mixing. This is due to the additive achieving a better balance among solute-solute, solute-solvent, and solvent-solvent interactions, indicating the potential for improvements in the Drude polarizable alcohol model.

### Keywords

molecular dynamics; electronic polarization; mixed solutions; partial molar volume; radial distribution function

## Introduction

Nowadays, computer simulations are utilized widely to study condense-phase systems and biopolymers. In these simulations the empirical force field (FF) used as part of an effective potential function for describing the intramolecular and intermolecular interactions is central to their accuracy and reliability. Traditional force fields for biomolecular simulations are based on additive, nonpolarizable models in which the nonbond terms in the potential functions are treated in a pairwise additive fashion.[1] In such models, the atomic charges are kept fixed such that induced polarization, which has been shown to be important in some cases, such as ion solvation[2] and ion selectivity in channels and transporters,[3, 4] is inherently missing and is only taken into account implicitly. Polarizable force fields, on the other hand, explicitly model induced polarization by adding extra electrostatic terms.[5, 6] Both additive and polarizable force fields are optimized by targeting various QM target data, including intramolecular geometries, vibrational spectra, dihedral potential energy scans, compound-water interactions, compound-rare gas interactions as well as experimental condensed-phase properties such as molecular volumes, heats of vaporization, and recently, free energies of hydration.[7–9] With the majority of force fields developed to date properties of liquid

*corresponding author: alex@outerbanks.umaryland.edu.

NIH-PA Author Manuscript
NIH-PA Author Manuscript
NIH-PA Author Manuscript

NIH-PA Author Manuscript

NIH-PA Author Manuscript

NIH-PA Author Manuscript

mixtures have not been included as experimental target data. Ideally, force fields optimized to reproduce properties of pure liquids have captured the essential characteristics of the molecules and should accurately model interactions among different molecular species. However, in practice, it has been shown such force fields often do not work very well for liquid mixtures without modifications.[10, 11]

Motivated to develop force fields that reproduce accurately not only pure liquid properties but also properties of liquid mixtures, Smith and coworkers created a set of united-atom additive force field models that reproduce experimental data analyzed by Kirkwood-Buff analysis.[12, 13] This includes Kirkwood-Buff integrals (KBIs), excess coordination numbers, partial molar volumes (PMVs), activity derivatives, excess Gibbs free energies etc. While this force field, termed the Kirkwood-Buff Derived Force Field (KBFF), does yield improved properties for liquid mixtures over additive force fields commonly used for biomolecular simulations, e.g. CHARMM,[14] Amber,[15] OPLS,[16] GROMOS[17] etc., it is not clear if it will be adopted widely by the simulation community. Accordingly, it is of interest to evaluate available biomolecular force fields using Kirkwood-Buff analysis to determine their accuracy as well as lay the groundwork for future optimization efforts.

Recently, we assessed the performance of both the CHARMM all-atom additive and Drude polarizable force fields in modeling aqueous amide solutions.[18] It was shown that while Kirkwood-Buff experimental data was not included as part of the target data during parameter optimization, the Drude polarizable force field better reproduced the studied liquid mixture KB data as compared to the CHARMM additive force field, with the biggest differences occurring at low solute concentrations. In the present study, we extended our evaluation of the CHARMM force fields to methanol and aqueous methanol as a model for alcohols including the 2'OH in RNA and the serine and threonine amino acid side chains.

Several other force fields for methanol have been developed,[9, 19–24] and a number of simulations on methanol and aqueous methanol solutions have been performed.[24–27] Among them, work from the Smith group has developed a united-atom additive model by reproducing the experimental KB integrals.[24] A nonadditive model developed by the Patel group showed reasonable agreement with the experimental KB integrals even when the integrals were not part of the target data during the force field development.[26] Our results in the present study demonstrate that both CHARMM additive and Drude polarizable force field reproduced the experimental KB integrals of methanol solutions reasonably well, though the potential for possible improvements in the model is noted.

## Methods

### Kirkwood-Buff Analysis of the Experimental Data

The Kirkwood-Buff integrals (KBI) are defined as,[28]

$$G_{ij}=\int_0^\infty [g_{ij}(r)-1]\cdot 4\pi r^2 dr. \quad (1)$$

where $g_{ij}(r)$ is the radial distribution function (RDF) in the grand canonical ensemble ($V$, $T$, μ) between species $i$ and $j$, and $G_{ij}$ is the corresponding KB integral.

For methanol cosolvent ($c$) and water ($w$) mixtures, given the experimental measurements of the partial molar volumes $\left(\overline{V}\right)$,[29] the isothermal compressibility ($\kappa_T$),[30] density (ρ), and excess molar Gibbs free energy $\left(G_m^E\right)$[31] of the solution, KBIs can be obtained as[32]

NIH-PA Author Manuscript

NIH-PA Author Manuscript

NIH-PA Author Manuscript

$$G_{cc}=kT\kappa_T-\frac{1}{\rho_c}+\frac{\rho_w\overline{V}_w^2\rho}{\rho_c D}, \quad (2)$$

$$G_{cw}=kT\kappa_T-\frac{\rho\overline{V}_w\overline{V}_c}{D}, \quad (3)$$

$$G_{ww}=kT\kappa_T-\frac{1}{\rho_w}+\frac{\rho_c\overline{V}_c^2\rho}{\rho_w D}, \quad (4)$$

where

$$\rho=\rho_w+\rho_c, \quad (5)$$

and

$$D=\frac{x_c}{kT}\left(\frac{\partial\mu_c}{\partial x_c}\right)_{T,P}=1+\frac{x_w x_c}{kT}\left(\frac{\partial^2 G_m^E}{\partial x_c^2}\right)_{T,P}. \quad (6)$$

$x_c$ and $x_w$ are the mole fraction of the cosolvent and water, $\rho_c$ and $\rho_w$ are the number density of the cosolvent and water, $G_m^E$ is the excess molar Gibbs free energy of the solution, $k$ is the Boltzmann constant, $T$ is the thermodynamic temperature. The second term in the definition of $D$ is often denoted as the activity derivative, $f_{cc}$, as follows:[33]

$$f_{cc}\equiv\frac{x_w x_c}{kT}\left(\frac{\partial^2 G_m^E}{\partial x_c^2}\right)_{T,P}. \quad (7)$$

## Molecular Dynamics Simulations of Aqueous Methanol Solutions

Empirical force field calculations were performed with the program CHARMM[34] utilizing both the additive CHARMM General force field[35] (CGenFF) and the Drude polarizable force field[5] at 300 K and 1 atm in the NPT ensemble. The TIP3P water model[36] was used for the additive FF simulations and the SWM4-NDP water model[37, 38] was used in all simulations involving the Drude model.

To simulate aqueous methanol solutions, a range of concentrations in terms of mole fraction were considered from pure water through mixed solutions to pure cosolvent. The initial configuration for each composition was prepared by randomly placing a certain number of methanol molecules in a cubic box then adding water molecules to match the concentrations listed in Table 1. All systems were then simulated to allow for extensive equilibration using the additive model. RDFs were computed as a function of simulation time, ensuring that the solutions were fully mixed as judged by the RDFs becoming constant (usually about 1 ns). Then 10 ns production simulations were performed at each concentration. For the additive simulations, extended system algorithms[39] and Nose-Hoover thermostat[40, 41] were used to modulate the pressure and temperature with the mass of the pressure piston set to 1000 a.m.u. and the mass of the thermal piston set to 2000 kcal/mol ps$^2$. Equations of motion were integrated using the Leap-Frog algorithm at a time step of 2 fs.

The final configurations from the additive simulations were used as starting configurations for the Drude simulations. A Nose-Hoover thermostat with a relaxation time of 0.1 ps was

NIH-PA Author Manuscript

NIH-PA Author Manuscript

NIH-PA Author Manuscript

applied to all the atoms to control the global temperature of the system at 300 K. A modified Andersen-Hoover barostat[40, 41] with a relaxation time of 0.1 ps was used to maintain the system at constant pressure. The extended Lagrangian double thermostat formalism[42] was used to control the amplitude of the oscillations of Drude particles with a separate low-temperature thermostat (at $T$ = 1 K) to ensure that their time course approximates the self-consistent field (SCF) regime. A relaxation time of 5 fs was used for the Drude oscillator thermostat. The force constant was set at 1000 kcal/(mol Å$^2$) for the Drude particle-parent atom harmonic terms. Simulations were performed for 11 ns using the velocity Verlet integrator at a time step of 1 fs, with the last 10 ns used for analyses.

In both the additive and Drude simulations, the Particle Mesh Ewald[43] method was used to evaluate the electrostatic interactions with a real space cutoff of 12 Å, a coupling parameter of 0.34 and a sixth-order spline for mesh interpolation. All nonbonded electrostatic interactions involving Drude particles are treated in the same way as electrostatic interactions between parent atoms while the nonbonded interactions are modified to allow 1–2 and 1–3 screened dipole-dipole interactions,[44] as proposed by Thole.[45] Lennard-Jones (LJ) interactions were switched off between 10 Å and 12 Å via vfswitch in the additive simulations and vswitch in the Drude simulations.[46, 47] Nonbonded pair lists were maintained up to 14 Å and updated heuristically. Isotropic long-range corrections to the LJ terms were applied.[48] All bonds involving hydrogens were constrained using SHAKE[49] for the additive simulations and using the SHAKE/Roll and RATTLE/Roll procedures[42] for the Drude simulations. Coordinates were saved every 1 ps for RDF computations and bulk property calculations.

Additional solution properties were calculated as follows. Solution density (ρ) is the total mass divided by the average volume of the simulation box $\langle V \rangle$:

$$\rho = \frac{\text{mass}}{\langle V \rangle}. \quad (8)$$

The excess coordination number $N_{ij}$ was computed by:

$$N_{ij} = \rho_j G_{ij}. \quad (9)$$

where $\rho_j$ is the number density of component $j$ and $G_{ij}$ is the Kirkwood-Buff integral. The molar enthalpy of mixing $\Delta H_m$ was calculated from the potential energy via[23]

$$\Delta H_m = U_m - x_c U_c - x_w U_w, \quad (10)$$

where $U_m$ is the potential energy of the mixture, $U_c$ and $U_w$ the potential energies of the pure cosolvent and water, respectively. The self-diffusion constant ($D_0$) was evaluated from the mean squared displacement of the center of mass (COM) of the respective cosolvent and water molecules under the Stokes Einstein relation,[50] with a system size correction as follows:[51]

$$D_{\text{PBC}} = \lim_{t \to \infty} \frac{1}{6t} \left\langle \frac{1}{N} \sum_{i=1}^{N} \left[ r_{\text{COM},i(t)} - r_{\text{COM},i(0)} \right]^2 \right\rangle, \quad (11)$$

$$D_0 = D_{\text{PBC}} + \frac{2.837297kT}{6\pi\eta L}, \quad (12)$$

where η is shear viscosity evaluated by the Green-Kubo relation[52, 53] from a separate NVT simulation, $L$ is the box length of the cubic simulation box determined at the proper density.

NIH-PA Author Manuscript

NIH-PA Author Manuscript

NIH-PA Author Manuscript

The dielectric constant was calculated from the dipole moment fluctuations using the following equation:[54, 55]

$$\varepsilon=\varepsilon_{\infty}+\frac{4\pi}{3\langle V\rangle kT}\left(\left\langle M^2\right\rangle-\langle M\rangle^2\right). \quad (13)$$

where $M$ is the total dipole moment of the simulation box. The high frequency optical dielectric constant, $\varepsilon_{\infty}$, was estimated from the Clausius-Mossotti equation[56] for the Drude model. For the additive simulations $\varepsilon_{\infty}$ was set to 1 since no electronic degrees of freedom were explicitly modeled. The isothermal compressibility could be evaluated from KBIs using equation (4) in theory but this approach is typically statistically unreliable. Instead it was calculated from[9, 57]

$$\kappa_T=-\frac{1}{V}\left(\frac{\partial V}{\partial P}\right)_T=\frac{\langle V^2\rangle}{\langle V\rangle kT}, \quad (14)$$

where $\langle V\rangle$ is the ensemble average of volume and $\langle V^2\rangle$ is the volume fluctuations. Errors were estimated by using five 2 ns blocks from which averages and standard errors were obtained.

## Kirkwood-Buff Analysis of the Simulated Data

The simulated Kirkwood Buff integrals (KBI) were approximated by[33]

$$G_{ij}=\int_0^{\infty}\left[g_{ij}(r)-1\right]\cdot 4\pi r^2 dr\approx\int_0^{R}\left[g_{ij}(r)-1\right]\cdot 4\pi r^2 dr. \quad (15)$$

where $R$ is the cutoff distance after which RDFs are essentially unity. Following the work of Smith and coworkers, the simulated KBIs were obtained by integrating the RDFs via the trapezoidal rule and averaging between 9.5 and 12.0 Å.[24] The choice of such a range is further justified from the reasonable agreements between the properties calculated from the simulated KBIs and the properties determined from experimental data through Kirkwood-Buff analysis, as shown below.

Using the simulated KBIs, the following properties can be determied and readily compared to those determined from the experimental data.[28, 33]

$$\overline{V}_c=\frac{1+\rho_w\left(G_{ww}-G_{cw}\right)}{\eta}, \quad (16)$$

$$\overline{V}_w=\frac{1+\rho_c\left(G_{cc}-G_{cw}\right)}{\eta}, \quad (17)$$

$$f_{cc}=\left(\frac{\partial\ln f_c}{\partial\ln x_c}\right)_{T,P}=-\frac{x_c\rho_w\Delta G}{1+x_c\rho_w\Delta G}, \quad (18)$$

where

$$\eta=\rho_w+\rho_c+\rho_w\rho_c\Delta G, \quad (19)$$

and

NIH-PA Author Manuscript

NIH-PA Author Manuscript

NIH-PA Author Manuscript

$$\Delta G = G_{cc} + G_{ww} - 2G_{cw}. \quad (20)$$

## Results and Discussion

A summary of the simulations performed on aqueous methanol solutions is presented in Table 1. As required for a complete Kirkwood-Buff analysis, the entire composition range from pure water through methanol/water mixture to pure methanol is covered. They were all simulated for 10 ns after 1 ns equilibration to ensure reasonable precision in the data. Beyond comparison of the CHARMM additive and polarizable FF results we also discuss previously reported results from the KBFF methanol simulations of Smith and coworkers,[24] as well as other published studies on methanol.

The oxygen-to-oxygen RDFs are displayed in Figure 1 as a function of mole fraction. Both the CHARMM additive and Drude force fields predicted increased solute-solute, solute solvent and solvent solvent interactions as the mole fraction increased. This is consistent with the findings from aqueous methanol solutions modeled by the KBFF.[24] For all three types of RDFs similar positions were obtained for the maxima and minima. This is not surprising considering that the chemical structures of methanol and water molecules are very similar. A closer look revealed that the Drude RDFs have slightly higher maxima and slightly lower minima in the first solvation shell. This is due to the similar but different charge distribution in both models and the introduction of induced polarization in the Drude model. The increase in the first water-to-water solvation shell suggested an increasing degree of water self association with the increasing methanol mole fraction, consistent with neutron diffraction data.[58]

The simulated KBIs calculated using equation (1) from the RDFs in Figure 1 are displayed in Figure 2 along with the experimental KBIs of aqueous methanol solutions computed from the experimental data from an inverse KB procedure.[32] As shown in Figure 2, the experimental KBIs were well reproduced over the entire concentration range by both the CHARMM additive and Drude force fields, except for a somewhat large overestimation for the additive $G_{cc}$ at $x_c = 0.125$. This is in contrast with our previous study on the aqueous amide solutions modeled by the CHARMM additive force field,[18] in which it was shown that there were significant overestimations for $G_{cc}$ and $G_{ww}$ as well as significant underestimations for $G_{cw}$ at low concentrations up to $x_c = 0.20$. This suggests that the quality of a force field in reproducing experimental data via Kirkwood-Buff analysis must be performed on a case by case basis for a force field, as the additive model can, to varying extents, model aqueous solutions. Indeed, the additive KBFF is able to reproduce the KB experimental data of aqueous methanol,[24] sodium chloride,[59] urea,[60] guanidinium chloride,[61] acetone,[62] as well as for other molecules,[11, 63, 64] when such experimental data were targeted during the force field optimization.

Excess coordination numbers via equation (9) shown in Figure 3 are another way to compare the simulated and experimental KBIs. The trends in the experimental data were well reproduced by both the CHARMM additive and Drude force fields. There was essentially quantitative agreement for $N_{cc}$ and $N_{cw}$ over the whole composition range, while $N_{ww}$ was underestimated at $x_c = 0.5$ and 0.675 for both force fields and at $x_c = 0.375$ for the Drude force field. The slight underestimation for $N_{ww}$ also exists in the KBFF methanol solutions. It is worth noting that the use of excess coordination numbers helps to suppress the inherent uncertainties in both the simulated and experimental KBIs at low $j$ concentrations.[24] This is especially true for the additive methanol solution at $x_c = 0.125$ where a relatively large overestimation of $G_{cc}$ is seen in Figure 2 but the agreement between the simulation results and the experiment data for its excess coordination number is

NIH-PA Author Manuscript

NIH-PA Author Manuscript

NIH-PA Author Manuscript

excellent. However, it should be kept in mind that the agreement may be due to cancellation of errors in evaluating both the solution density and the KBI. When other properties such as partial molar volumes and activity derivatives are calculated from the KBIs, the deviations in the accuracy of KBIs will manifest themselves again, as shown below.

The simulated and experimental densities, partial molar volumes, and excess molar volumes are presented in Figure 4. The density of pure additive methanol was slightly underestimated and consequently there was a gradually increasing deviation from the experimental density as the mole fraction increased. This was observed in other additive methanol models,[24, 65] while an overestimation was observed for GAFF (General Amber Force Field).[66] In contrast, the density of pure Drude methanol is improved as compared to its additive counterpart. As a result, the density of aqueous methanol solutions modeled by the Drude FF displayed an improved agreement with the experimental density. For partial molar volumes, both the methanol and water PMVs were quantitatively reproduced by the Drude FF, however, there was a consistent overestimation of the additive FF for the methanol PMV and a slight overestimation at high mole fractions for the water PMV. With better reproduction of both density and partial molar volumes for the Drude model over the additive model, it is not surprising that the excess molar volumes of the solutions showed better agreement for the Drude model with the experimental data as well. The overall agreement in Figure 4 with the experimental data is comparable for the additive methanol model and superior for the Drude methanol model to that of KBFF methanol solutions.[24] It is worth emphasizing that the reasonable agreement between the partial molar volumes calculated from the simulated KBIs and those from the experimental KBIs suggests that the averaging of KBIs between 9.5 and 12 Å captured the essential quantitative characteristics of the integrals. Care must be taken when selecting the distance for averaging as the calculated KBIs may potentially deviate from the experimental values if the averaging was done over the long tails of the RDFs where numerical uncertainties exist, which are magnified by the volume factor in equation (15).

Activity derivatives, $f_{cc}$, were obtained from simulated KBIs using equation (18). Then by fitting $f_{cc}$ with the Redlich Kister equation,[67] one can obtain the excess molar Gibbs energy. The results are displayed in Figure 5. The oscillating behavior in $f_{cc}$ was relatively well reproduced by the additive model but the Drude model predicted a more flat $f_{cc}$ compared to the experimental data. The variation of excess molar Gibbs energy was also well reproduced by the additive model at medium and high concentrations, although there was a slight overestimation at the low concentrations. The Drude model underestimated the excess molar Gibbs energy over the entire composition range. The result came as a surprise because the Drude model showed improvements over the additive model in terms of KBIs, solution densities, PMVs etc. Accordingly, one would expect the Drude model to perform better with the activity derivative and excess molar Gibbs energy as well. Indeed, our previous study on aqueous amide solutions showed improvement for the Drude model over the additive model in these properties.[18] A deeper analysis revealed that although the Drude model better reproduced experimental results in terms of the absolute values of KBIs than the additive model, according to equations (18) and (20), it is the difference of KBIs, ΔG, that plays a more important role in evaluating the activity derivative. The additive model achieved a better balance in computing ΔG that involved all three kinds of KBIs, therefore, a better activity derivative and excess molar Gibbs energy was obtained as compared to the experimental data. Another possible reason for the better performance of the additive model is its ability of obtaining better energetics in terms of excess molar enthalpy of mixing, calculated by employing equation (10) and shown in the bottom panel of Figure 5. The simulated enthalpy was less favorable up to $x_c = 0.6$ for the additive model and much more favorable beyond $x_c = 0.15$ for the Drude model compared to the experimental data.[68] The same overestimation was also observed for aqueous methanol solutions modeled by the

NIH-PA Author Manuscript

NIH-PA Author Manuscript

NIH-PA Author Manuscript

additive OPLS force field[65] and the polarizable force field based on charge equilibrium formulism.[25] Energetic deviations as such would certainly impact the solution structures during the simulations and thus, impact the RDFs as shown in Figure 1 and ultimately all the Kirkwood-Buff analyses followed by evaluating KBIs from the RDFs. In our previous study on aqueous amide solutions, the Drude model achieved better excess molar enthalpy than the additive model and also improved activity derivatives.[18] Considering that it is the opposite in the present study, it is possible that an accurate evaluation of excess molar enthalpy is a prerequisite for an accurate activity derivative and, therefore, an accurate excess molar Gibbs energy. More work needs to be done to verify this hypothesis in future force field development and refinement efforts.

The concentration-dependent diffusion constants of both methanol and water calculated from equations (11) and (12) are displayed in Figure 6. The experimental trends were reproduced only qualitatively by the CHARMM additive model, with similar behavior being reported for the additive OPLS model,[65] but quantitatively by the Drude model. For a neat methanol solution, both additive and Drude models overestimated the diffusion constants, with the deviation somewhat less for the Drude model. However, the diffusion constants of the Drude model quickly approached the experimental data as the concentration decreased while those of the additive model were consistently overestimated. The diffusion constants of the SWM4-NDP water over the entire composition range were excellent compared to the experimental data while those of the TIP3P water were consistently overestimated. This is a direct outcome of force field parametrization where the diffusion constant for the SWM4-NDP water model is in good agreement with experiment while that for the TIP3P water model is markedly overestimated.[37]

The isothermal compressibilities and the dielectric constants of the aqueous methanol solutions are displayed in Figure 7. Essentially quantitative agreement with experiment[71] was observed with a few exceptions as follows. The isothermal compressibility of the TIP3P water was slightly overestimated while that of the additive methanol model was in excellent agreement with experiment.[9] As a result, the isothermal compressibilities of the solutions were also slightly overestimated at the low concentrations but were nicely reproduced at the medium and high concentrations. The same was true for the Drude model except that the somewhat large underestimation was due to the isothermal compressibility of the pure methanol. The dielectric constant of the TIP3P water model was largely overestimated also as a direct consequence of its parametrization.[37] However, the dielectric constant of the additive methanol was only slightly underestimated. Therefore, the dielectric constants of the solutions were in better agreement with experiment as the concentration increased. It is not surprising that the dielectric constants of the Drude solutions were excellent relative to experiment[72] since both those of the pure SWM4-NDP water and pure methanol reproduced the experimental data very well from their parametrizations.[9] It also outperformed its other additive counterparts such as OPLS and GAFF.[66] The results in Figure 7 emphasize that the solution properties of liquid mixtures can only be as good as those of their components. It is therefore important to obtain bulk properties of pure liquids that reproduce experimental results very well during the force field development in order to describe their mixed solution properties correctly.

## Conclusions

Kirkwood-Buff analysis was performed on aqueous methanol solutions modeled by both the CHARMM additive and Drude polarizable force fields. It was shown that both models reproduced the experimental KBIs and excess coordination numbers adequately well over the entire concentration range. This is in contrast to the additive N-methylacetamide model we previously investigated, in which significant deviations were observed for these two

NIH-PA Author Manuscript

NIH-PA Author Manuscript

NIH-PA Author Manuscript

properties by the additive force field,[18] whereas the Drude model performed very favorably compared to the experimental data. Notably, in the present study the additive model performed better than the Drude model in reproducing activity derivative, excess molar Gibbs energy and excess molar enthalpy of mixing. This is due to the ability of the additive to more accurately treat the difference of KBIs, $\Delta G$, as compared to the Drude model, even though the Drude model obtained better KBIs in terms of absolute values. Considering that the additive model reproduced the excess molar enthalpy of mixing better than the Drude model and the associated impact on the solution structures, it is suggested that including energetics of the mixed solutions as target data during force field development would improve the performance of the model in describing activity derivative and excess molar Gibbs energy.

The Drude model showed significant improvement over the additive model in solution densities, partial molar volumes, excess molar volumes, concentration-dependent diffusion constants, and dielectric constants. The isothermal compressibilities from both models are comparable. A closer look at these results showed that the concentration-dependent solution properties could only be as good as the bulk properties of the pure liquids. It is therefore vital to obtain accurate bulk properties of pure liquids in order to have an accurate description of solution mixed by them.

The poorer agreement of the Drude model versus the additive force field for the activity derivative and excess molar Gibbs energy was unexpected. As these properties are dominated by the balance between the solvent-solvent, solvent-solute and solute-solute interactions this may be related to the absence of lone pairs on the SWM4 water model which are present on the Drude alcohols. This may lead to a slight imbalance in the three types of interactions that are better treated in the additive model, which lacks lone pairs for all molecules. To test this hypothesis, KBI calculations on the Drude model using the recently developed SWM6 water model,[55] which includes lone pairs could be undertaken.

Another possible approach to facilitate improved reproduction of the activity derivative and excess molar Gibbs energy by the Drude model, as well as other observables, would be optimization of the Thole scaling factor.[45] This term impacts the strength of the 1,2 and 1,3 dipole-dipole interactions present in the Drude model, thereby improving treatment of the molecular polarizability. During the development of the Drude alcohol parameters, the Thole scaling factor was constrained to a value of 1.3, originally optimized for benzene. Subsequent work on the Drude model showed the importance of including atom-based Thole scaling factors in the model.[44] Accordingly, inclusion of such terms is anticipated to lead to improvements in the Drude polarizable model that may overcome limitations observed in this study. This and potential improvements associated with the use of the SWM6 model[55] will be investigated in a future study.

## Acknowledgments

Financial support from the NIH (GM051501 and GM072558) is acknowledged.

## References

(1). Mackerell AD Jr. Empirical Force Fields for Biological Macromolecules: Overview and Issues. J. Comput. Chem. 2004; 25:1584–1604. [PubMed: 15264253]

(2). Luo Y, Jiang W, Yu HB, Mackerell AD Jr. Roux B. Simulation Study of Ion Pairing in Concentrated Aqueous Salt Solutions with a Polarizable Force Field. Faraday Discuss. 2013; 160:135–149. [PubMed: 23795497]

(3). Roux B, Berneche S, Egwolf B, Lev B, Noskov SY, Rowley CN, Yu HB. Ion Selectivity in Channels and Transporters. J. Gen. Physiol. 2011; 137:415–426. [PubMed: 21518830]

NIH-PA Author Manuscript

NIH-PA Author Manuscript

NIH-PA Author Manuscript

(4). Warshel A, Kato M, Pisliakov AV. Polarizable Force Fields: History, Test Cases, and Prospects. J. Chem. Theory Comput. 2007; 3:2034–2045.

(5). Lopes PEM, Roux B, Mackerell AD Jr. Molecular Modeling and Dynamics Studies with Explicit Inclusion of Electronic Polarizability: Theory and Applications. Theor. Chem. Acc. 2009; 124:11–28. [PubMed: 20577578]

(6). Zhu X, Lopes PEM, MacKerell AD Jr. Recent Developments and Applications of the Charmm Force Fields. WIREs Comput. Mol. Sci. 2012; 2:167–185.

(7). Vorobyov I, Anisimov VM, Greene S, Venable RM, Moser A, Pastor RW, MacKerell AD Jr. Additive and Classical Drude Polarizable Force Fields for Linear and Cyclic Ethers. J. Chem. Theory Comput. 2007; 3:1120–1133.

(8). Vorobyov IV, Anisimov VM, MacKerell AD Jr. Polarizable Empirical Force Field for Alkanes Based on the Classical Drude Oscillator Model. J. Phys. Chem. B. 2005; 109:18988–18999. [PubMed: 16853445]

(9). Anisimov VM, Vorobyov IV, Roux B, Mackerell AD Jr. Polarizable Empirical Force Field for the Primary and Secondary Alcohol Series Based on the Classical Drude Model. J. Chem. Theory Comput. 2007; 3:1927–1946. [PubMed: 18802495]

(10). Chitra R, Smith PE. A Comparison of the Properties of 2,2,2-Trifluoroethanol and 2,2,2-Trifluoroethanol/Water Mixtures Using Different Force Fields. J. Chem. Phys. 2001; 115:5521–5530.

(11). Kang M, Smith PE. A Kirkwood-Buff Derived Force Field for Amides. J. Comput. Chem. 2006; 27:1477–1485. [PubMed: 16823811]

(12). Pierce V, Kang M, Aburi M, Weerasinghe S, Smith PE. Recent Applications of Kirkwood-Buff Theory to Biological Systems. Cell Biochem. Biophys. 2008; 50:1–22. [PubMed: 18043873]

(13). Smith, PE.; Matteoli, E.; O'Connell, JP. Fluctuation Theory of Solutions : Applications in Chemistry, Chemical Engineering, and Biophysics. CRC Press; Boca Raton, FL: 2013.

(14). Mackerell AD Jr. Bashford D, Bellott M, Dunbrack RL, Evanseck JD, Field MJ, Fischer S, Gao J, Guo H, Ha S, et al. All-Atom Empirical Potential for Molecular Modeling and Dynamics Studies of Proteins. J. Phys. Chem. B. 1998; 102:3586–3616.

(15). Ponder JW, Case DA. Force Fields for Protein Simulations. Adv. Protein Chem. 2003; 66:27–85. [PubMed: 14631816]

(16). Kaminski GA, Friesner RA, Tirado-Rives J, Jorgensen WL. Evaluation and Reparametrization of the OPLS-AA Force Field for Proteins via Comparison with Accurate Quantum Chemical Calculations on Peptides. J. Phys. Chem. B. 2001; 105:6474–6487.

(17). Christen M, Hunenberger PH, Bakowies D, Baron R, Burgi R, Geerke DP, Heinz TN, Kastenholz MA, Krautler V, Oostenbrink C, et al. The Gromos Software for Biomolecular Simulation: GROMOS05. J. Comput. Chem. 2005; 26:1719–1751. [PubMed: 16211540]

(18). Lin B, Lopes PEM, Roux B, Mackerell AD Jr. Kirkwood-Buff Analysis of Aqueous N-Methylacetamide and Acetamide Solutions Modeled by the CHARMM Additive and Drude Polarizable Force Fields. J. Chem. Phys. 2013 accepted.

(19). Caldwell JW, Kollman PA. Structure and Properties of Neat Liquids Using Nonadditive Molecular Dynamics: Water, Methanol, and N-Methylacetamide. J. Phys. Chem. 1995; 99:6208–6219.

(20). Dang LX, Chang T-M. Many-Body Interactions in Liquid Methanol and Its Liquid/Vapor Interface: A Molecular Dynamics Study. J. Chem. Phys. 2003; 119:9851–9857.

(21). Jorgensen WL, Maxwell DS, Tirado-Rives J. Development and Testing of the OPLS All-Atom Force Field on Conformational Energetics and Properties of Organic Liquids. J. Am. Chem. Soc. 1996; 118:11225–11236.

(22). Patel S, Brooks CL 3rd. A Nonadditive Methanol Force Field: Bulk Liquid and Liquid-Vapor Interfacial Properties via Molecular Dynamics Simulations Using a Fluctuating Charge Model. J. Chem. Phys. 2005; 122:024508. [PubMed: 15638599]

(23). Walser R, Mark AE, van Gunsteren WF, Lauterbach M, Wipff G. The Effect of Force-Field Parameters on Properties of Liquids: Parametrization of a Simple Three-Site Model for Methanol. J. Chem. Phys. 2000; 112:10450–10459.

NIH-PA Author Manuscript

NIH-PA Author Manuscript

NIH-PA Author Manuscript

(24). Weerasinghe S, Smith PE. A Kirkwood-Buff Derived Force Field for Methanol and Aqueous Methanol Solutions. J. Phys. Chem. B. 2005; 109:15080–15086. [PubMed: 16852908]

(25). Zhong Y, Warren GL, Patel S. Thermodynamic and Structural Properties of Methanol-Water Solutions Using Nonadditive Interaction Models. J. Comput. Chem. 2008; 29:1142–1152. [PubMed: 18074339]

(26). Zhong Y, Patel S. Nonadditive Empirical Force Fields for Short-Chain Linear Alcohols: Methanol to Butanol. Hydration Free Energetics and Kirkwood-Buff Analysis Using Charge Equilibration Models. J. Phys. Chem. B. 2010; 114:11076–11092. [PubMed: 20687517]

(27). Noskov SY, Kiselev MG, Kolker AM, Rode BM. Structure of Methanol-Methanol Associates in Dilute Methanol-Water Mixtures from Molecular Dynamics Simulation. J. Mol. Liq. 2001; 91:157–165.

(28). Kirkwood JG, Buff FP. The Statistical Mechanical Theory of Solutions. I. J. Chem. Phys. 1951; 19:774–777.

(29). Douheret G, Khadir A, Pal A. Thermodynamic Characterization of the Water + Methanol System, at 298.15k. Thermochim. Acta. 1989; 142:219–243.

(30). Handbook of Chemistry and Physics. 93rd Edition. 2012–2013.

(31). Butler JAV, Thomson DW, Maclennan WH. 173. The Free Energy of the Normal Aliphatic Alcohols in Aqueous Solution. Part I. The Partial Vapour Pressures of Aqueous Solutions of Methyl, N-Propyl, and N-Butyl Alcohols. Part II. The Solubilities of Some Normal Aliphatic Alcohols in Water. Part III. The Theory of Binary Solutions, and Its Application to Aqueous-Alcoholic Solutions. J. Chem. Soc. 1933:674–686.

(32). Ben-Naim A. Inversion of the Kirkwood--Buff Theory of Solutions: Application to the Water--Ethanol System. J. Chem. Phys. 1977; 67:4884–4890.

(33). Ben-Naim, A. Molecular Theory of Solutions. Oxford University Press; Oxford; New York: 2006.

(34). Brooks BR, Brooks CL, Mackerell AD Jr. Nilsson L, Petrella RJ, Roux B, Won Y, Archontis G, Bartels C, Boresch S, et al. CHARMM: The Biomolecular Simulation Program. J. Comput. Chem. 2009; 30:1545–1614. [PubMed: 19444816]

(35). Vanommeslaeghe K, Hatcher E, Acharya C, Kundu S, Zhong S, Shim J, Darian E, Guvench O, Lopes P, Vorobyov I, et al. CHARMM General Force Field: A Force Field for Drug-Like Molecules Compatible with the CHARMM All-Atom Additive Biological Force Fields. J. Comput. Chem. 2010; 31:671–690. [PubMed: 19575467]

(36). Jorgensen WL, Chandrasekhar J, Madura JD, Impey RW, Klein ML. Comparison of Simple Potential Functions for Simulating Liquid Water. J. Chem. Phys. 1983; 79:926–935.

(37). Lamoureux G, Harder E, Vorobyov IV, Roux B, Mackerell AD Jr. A Polarizable Model of Water for Molecular Dynamics Simulations of Biomolecules. Chem. Phys. Lett. 2006; 418:245–249.

(38). Lamoureux G, Mackerell AD Jr. Roux B. A Simple Polarizable Model of Water Based on Classical Drude Oscillators. J. Chem. Phys. 2003; 119:5185–5197.

(39). Feller SE, Zhang YH, Pastor RW, Brooks BR. Constant Pressure Molecular Dynamics Simulation: the Langevin Piston Method. J. Chem. Phys. 1995; 103:4613–4621.

(40). Nosé S. A Molecular Dynamics Method for Simulations in the Canonical Ensemble. Mol. Phys. 1984; 52:255–268.

(41). Hoover WG. Canonical Dynamics: Equilibrium Phase-Space Distributions. Phys. Rev. A. 1985; 31:1695–1697. [PubMed: 9895674]

(42). Lamoureux G, Roux B. Modeling Induced Polarization with Classical Drude Oscillators: Theory and Molecular Dynamics Simulation Algorithm. J. Chem. Phys. 2003; 119:3025–3039.

(43). Darden T, York D, Pedersen L. Particle Mesh Ewald: An N·Log(N) Method for Ewald Sums in Large Systems. J. Chem. Phys. 1993; 98:10089–10092.

(44). Harder E, Anisimov VM, Whitfield TW, Mackerell AD Jr. Roux B. Understanding the Dielectric Properties of Liquid Amides from a Polarizable Force Field. J. Phys. Chem. B. 2008; 112:3509–3521. [PubMed: 18302362]

(45). Thole BT. Molecular Polarizabilities Calculated with a Modified Dipole Interaction. Chem. Phys. 1981; 59:341–350.

NIH-PA Author Manuscript

NIH-PA Author Manuscript

NIH-PA Author Manuscript

(46). Steinbach PJ, Brooks BR. New Spherical-Cutoff Methods for Long-Range Forces in Macromolecular Simulation. J. Comput. Chem. 1994; 15:667–683.

(47). van der Spoel D, van Maaren PJ. The Origin of Layer Structure Artifacts in Simulations of Liquid Water. J. Chem. Theory Comput. 2005; 2:1–11.

(48). Allen, MPTDJ. Computer Simulation of Liquids. Clarendon Press ; Oxford University Press; Oxford [England]; New York: 1987.

(49). Ryckaert J-P, Ciccotti G, Berendsen HJC. Numerical Integration of the Cartesian Equations of Motion of a System with Constraints: Molecular Dynamics of N-Alkanes. J. Comput. Phys. 1977; 23:327–341.

(50). Einstein A. Über Die Von Der Molekularkinetischen Theorie Der Wärme Geforderte Bewegung Von in Ruhenden FlÜssigkeiten Suspendierten Teilchen. Annalen der Physik. 1905; 322:549–560.

(51). Yeh IC, Hummer G. System-Size Dependence of Diffusion Coefficients and Viscosities from Molecular Dynamics Simulations with Periodic Boundary Conditions. J. Phys. Chem. B. 2004; 108:15873–15879.

(52). Green MS. Markoff Random Processes and the Statistical Mechanics of Time-Dependent Phenomena. II. Irreversible Processes in Fluids. J. Chem. Phys. 1954; 22:398–413.

(53). Kubo R. Statistical-Mechanical Theory of Irreversible Processes. I. General Theory and Simple Applications to Magnetic and Conduction Problems. J. Phys. Soc. Jpn. 1957; 12:570–586.

(54). Gereben O, Pusztai L. On the Accurate Calculation of the Dielectric Constant from Molecular Dynamics Simulations: The Case of SPC/E and SWM4-DP Water. Chem. Phys. Lett. 2011; 507:80–83.

(55). Yu W, Lopes PEM, Roux B, MacKerell AD Jr. Six-Site Polarizable Model of Water Based on the Classical Drude Oscillator. J. Chem. Phys. 2013; 138

(56). Rysselberghe PV. Remarks Concerning the Clausius-Mossotti Law. J. Phys. Chem. 1931; 36:1152–1155.

(57). Mulero A, Faundez CA, Parra MI, Cuadros F. Theoretical Calculations of the Isothermal Compressibility for Simple Fluids. Thermochim. Acta. 1999; 334:1–15.

(58). Dixit S, Crain J, Poon WCK, Finney JL, Soper AK. Molecular Segregation Observed in a Concentrated Alcohol-Water Solution. Nature. 2002; 416:829–832. [PubMed: 11976678]

(59). Weerasinghe S, Smith PE. A Kirkwood-Buff Derived Force Field for Sodium Chloride in Water. J. Chem. Phys. 2003; 119:11342–11349.

(60). Weerasinghe S, Smith PE. A Kirkwood-Buff Derived Force Field for Mixtures of Urea and Water. J. Phys. Chem. B. 2003; 107:3891–3898.

(61). Weerasinghe S, Smith PE. A Kirkwood-Buff Derived Force Field for the Simulation of Aqueous Guanidinium Chloride Solutions. J. Chem. Phys. 2004; 121:2180–2186. [PubMed: 15260772]

(62). Weerasinghe S, Smith PE. Kirkwood-Buff Derived Force Field for Mixtures of Acetone and Water. J. Chem. Phys. 2003; 118:10663–10670.

(63). Bentenitis N, Cox NR, Smith PE. A Kirkwood-Buff Derived Force Field for Thiols, Sulfides, and Disulfides. J. Phys. Chem. B. 2009; 113:12306–12315. [PubMed: 19681588]

(64). Ploetz EA, Smith PE. A Kirkwood-Buff Force Field for the Aromatic Amino Acids. Phys. Chem. Chem. Phys. 2011; 13:18154–18167. [PubMed: 21931889]

(65). Wensink EJW, Hoffmann AC, van Maaren PJ, van der Spoel D. Dynamic Properties of Water/Alcohol Mixtures Studied by Computer Simulation. J. Chem. Phys. 2003; 119:7308–7317.

(66). Caleman C, Van Maaren P, Hong M, Hub JS, Costa L, van der Spoel D. Force Field Benchmark of Organic Liquids: Density, Enthalpy of Vaporization, Heat Capacities, Surface Tension, Isothermal Compressibility, Volumetric Expansion Coefficient, and Dielectric Constant. J. Chem. Theory Comput. 2012; 8:61–74. [PubMed: 22241968]

(67). Redlich O, Kister AT. Algebraic Representation of Thermodynamic Properties and the Classification of Solutions. Ind. Eng. Chem. 1948; 40:345–348.

(68). Benjamin L, Benson GC. A Deuterium Isotope Effect on the Excess Enthalpy of Methanol-water Solutions. J. Phys. Chem. 1963; 67:858–861.

NIH-PA Author Manuscript

NIH-PA Author Manuscript

NIH-PA Author Manuscript

(69). Derlacki ZJ, Easteal AJ, Edge AVJ, Woolf LA, Roksandic Z. Diffusion Coefficients of Methanol and Water and the Mutual Diffusion Coefficient in Methanol-Water Solutions at 278 and 298 K. J. Phys. Chem. 1985; 89:5318–5322.

(70). Woolf LA. Insights into Solute-Solute-Solvent Interactions from Transport Property Measurements with Particular Reference to Methanol-Water Mixtures and Their Constituents. Pure Appl. Chem. 1985; 57:1083–1090.

(71). Easteal AJ, Woolf LA. (P, Vm, T, X) Measurements for [(1 − x)H2O+xCH3OH] in the Range 278 to 323 K and 0.1 to 280 Mpa I. Experimental Results, Isothermal Compressibilities, Thermal Expansivities, and Partial Molar Volumes. J. Chem. Thermodyn. 1985; 17:49–62.

(72). Smith RL, Lee SB, Komori H, Arai K. Relative Permittivity and Dielectric Relaxation in Aqueous Alcohol Solutions. Fluid Phase Equilib. 1998; 144:315–322.

NIH-PA Author Manuscript

NIH-PA Author Manuscript

NIH-PA Author Manuscript

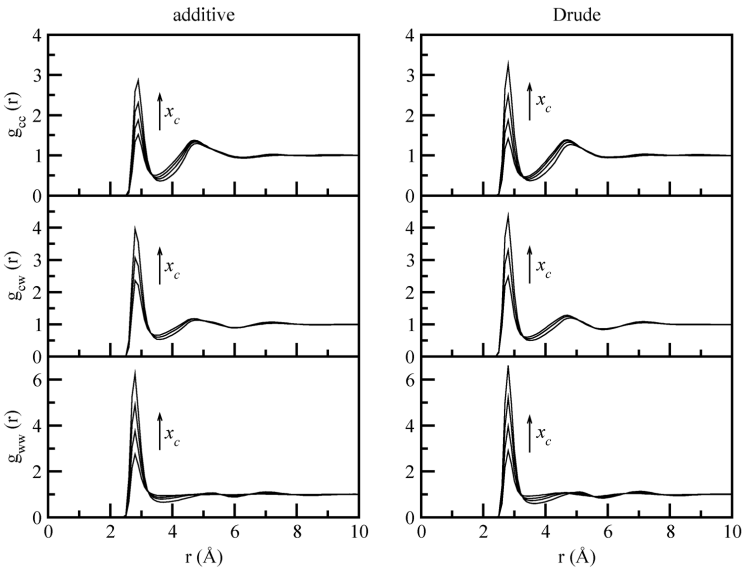


**Figure 1.**
The oxygen-to-oxygen radial distribution functions of aqueous methanol solutions. Mole fractions of 0.0, 0.25, 0.50, 0.75, and 1.0 are displayed.

NIH-PA Author Manuscript
NIH-PA Author Manuscript
NIH-PA Author Manuscript



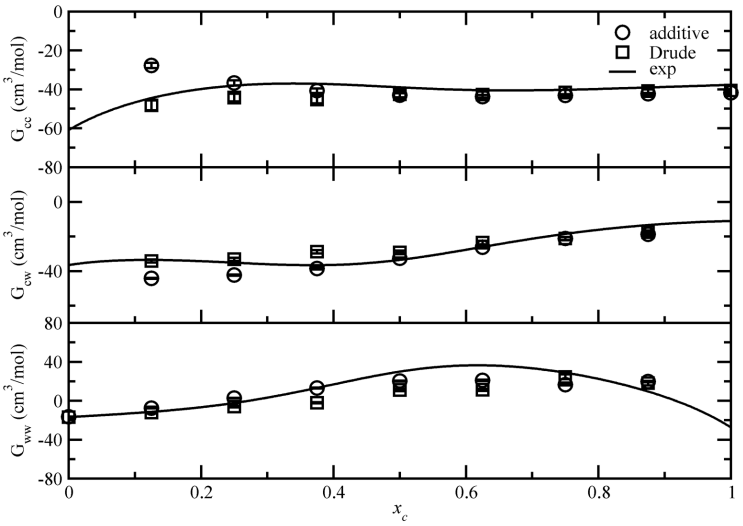


**Figure 2.**
Kirkwood-Buff integrals as a function of mole fraction for the aqueous methanol solutions.

NIH-PA Author Manuscript

NIH-PA Author Manuscript

NIH-PA Author Manuscript

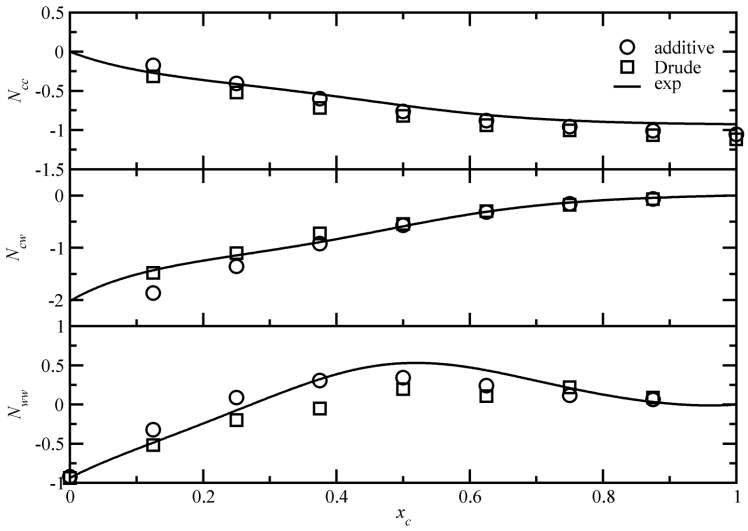


**Figure 3.**
Excess coordination numbers ($N_{ij}\rho_j G_{ij}$) as a function of methanol mole fraction.

NIH-PA Author Manuscript

NIH-PA Author Manuscript

NIH-PA Author Manuscript

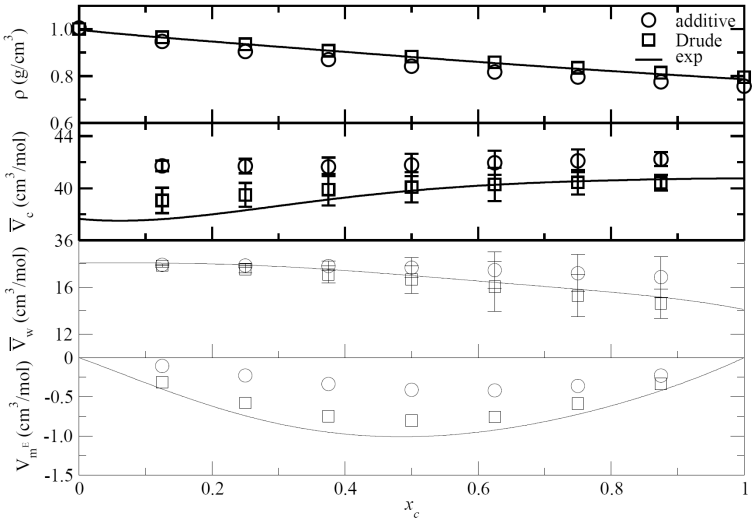


**Figure 4.**

The density (ρ), partial molar volumes of methanol ($V_C$) and water ($V_W$), and excess molar volume as a function of methanol mole fraction ($V_m$).

NIH-PA Author Manuscript

NIH-PA Author Manuscript

NIH-PA Author Manuscript

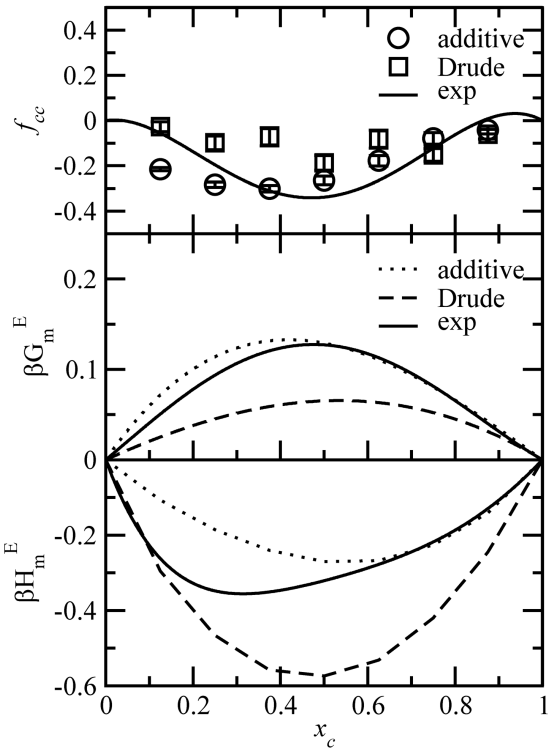


**Figure 5.**

The activity derivative ($f_{cc}$), excess molar Gibbs energy $\left(G_m^E\right)$, and excess molar enthalpy of mixing $\left(H_m^E\right)$ as a function of methanol mole fraction.

NIH-PA Author Manuscript

NIH-PA Author Manuscript

NIH-PA Author Manuscript

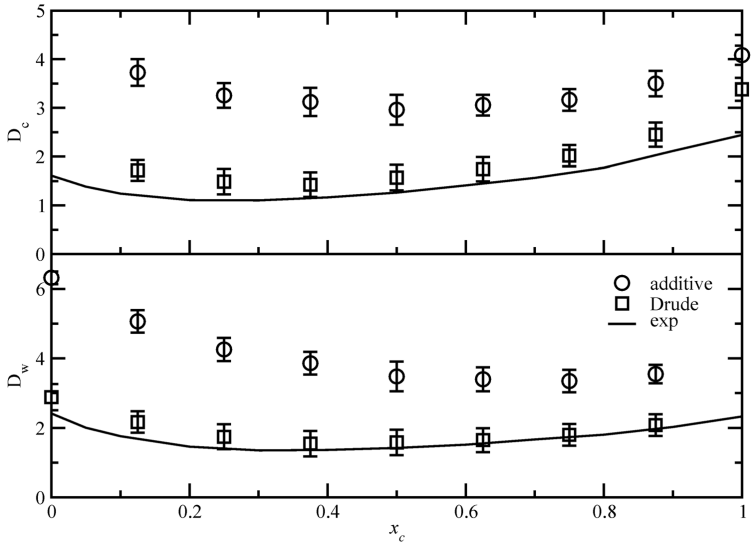


**Figure 6.**

Methanol and water diffusion constant ($10^{-5}$ $cm^2/s$) as a function of methanol mole fraction. The experimental results have been scaled to correct for isotropic effects.[69, 70]

NIH-PA Author Manuscript

NIH-PA Author Manuscript

NIH-PA Author Manuscript

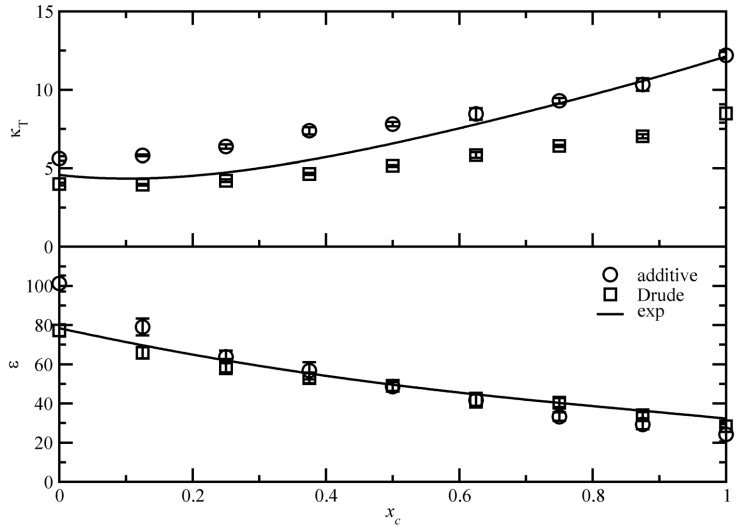


**Figure 7.**
The isothermal compressibilities ($10^{-5}$ $atm^{-1}$) and the dielectric constants as a function of methanol mole fraction compared to the experimental data.[71, 72]

NIH-PA Author Manuscript

NIH-PA Author Manuscript

NIH-PA Author Manuscript

## Table 1

Summary of the Methanol and Water Simulations[a]

| | | | additive | | | Drude | | |
|---|---|---|---|---|---|---|---|---|
| $x_c$ | $N_c$ | $N_w$ | $V$ (nm3) | $\rho_c$ (M) | ρ (g/cm3) | $V$ (nm3) | $\rho_c$ (M) p | ρ (g/cm3) |
| 0.0 | 0 | 2000 | 59.55 | 0.0 | 1.005 | 59.85 | 0.0 | 1.000 |
| 0.125 | 250 | 1750 | 69.33 | 6.0 | 0.947 | 68.05 | 6.1 | 0.965 |
| 0.250 | 500 | 1500 | 79.05 | 10.5 | 0.904 | 76.44 | 10.9 | 0.935 |
| 0.375 | 750 | 1250 | 88.82 | 14.0 | 0.870 | 85.12 | 14.6 | 0.908 |
| 0.500 | 1000 | 1000 | 98.71 | 16.8 | 0.842 | 94.19 | 17.6 | 0.883 |
| 0.625 | 1250 | 750 | 108.81 | 19.1 | 0.817 | 103.61 | 20.0 | 0.859 |
| 0.750 | 1500 | 500 | 119.13 | 20.9 | 0.796 | 113.42 | 22.0 | 0.836 |
| 0.875 | 1750 | 250 | 129.70 | 22.4 | 0.776 | 123.51 | 23.5 | 0.814 |
| 1.0 | 2000 | 0 | 140.59 | 23.6 | 0.757 | 133.88 | 24.8 | 0.795 |

[a]All simulations were performed for 10 ns at 300 K and 1 atm in the NPT ensemble.